

¹This problem has been treated for the case $n=2$ by B. R. Mollow, *Phys. Rev. A* **4**, 1666 (1971).

²A perturbation theory analysis of multiphoton processes may be found in W. Heitler, *The Quantum Theory of Radiation*, 3rd ed. (Clarendon, Oxford, England, 1957), Chap. 4.

³Multiphoton absorption from weak quantum-mechanical fields with arbitrary statistics has been discussed by B. R. Mollow, *Phys. Rev.* **175**, 1555 (1968); G. S. Agarwal, *Phys. Rev. A* **1**, 1445 (1970).

⁴A. Gold and P. Hernandez, *Phys. Rev.* **139**, A2002 (1965).

⁵T. Oka and T. Shimizu, *Phys. Rev. A* **2**, 587 (1970),

have observed strong (microwave) 2-photon excitations in inversion nonsymmetric cases. In their analysis of the problem, the effect of states other than the resonantly coupled pair is ignored. This approximation requires a special justification, since in general the contribution of other states to the effective coupling constant is comparable to that of the original pair, unless the other states are very far away in energy or are weakly coupled by the dipole-moment operator to both states of the resonantly coupled pair.

⁶R. Karplus and J. Schwinger, *Phys. Rev.* **73**, 1020 (1948).

Analog of the dc Josephson Effect in Superfluid Helium

J. P. Hulin, C. Laroche, A. Libchaber, and B. Perrin

Groupe de Physique des Solides, Ecole Normale Supérieure, Paris 5, France

(Received 2 August 1971)

An experiment is described in which we study the flow of helium through a 20- μ orifice which connects two helium baths. Closed capacitors are used to measure the helium level. Flow-gravitational-head difference characteristics are traced for various temperatures from 1.15 to 2.26 K. Subcritical and supercritical flow are clearly observed, and the effect of temperature on the relation between the chemical potential and the level difference is discussed. Abrupt appearance of supercritical flow is observed. With a quartz transducer placed in front of the coupling hole, a decrease and subsequent increase of the flow velocity with quartz voltage is measured.

I. INTRODUCTION

We report here various experiments on the flow of superfluid helium between two baths through a small hole (20 μ diam and 15 μ thickness). This setup approximates a Josephson junction. In such, a weak link, pressure gradients, vortex motion, and phase variations are localized in the very small volume of the hole and its vicinity. Richards, and later Khorana, have used this coupling system for a clear experimental study of the ac Josephson effect¹⁻⁴; their experiment showed that the vortex motion through the hole has an average frequency related to the chemical-potential difference $h\nu = mg\Delta z$, where Δz is the helium-level difference between the two baths; this motion is synchronized by a quartz transducer. Their results tend to indicate that there is no independent movement of vortices across the hole, which thus acts as a reasonable Josephson weak link.

Other flow experiments through thin channels have been reported, using either powders,⁵⁻⁷ long and narrow slits,^{8,9} or long capillaries¹⁰; in all these systems vortex motion may appear randomly in different parts of the channel, and the phase variation of the order parameter cannot be simply ana-

lyzed.

In our experiments with thin holes, we have studied the superfluid flow under zero chemical potential, the appearance of a critical velocity, and the variation of the dc current with a gravitational chemical-potential difference.

These experiments have been done at various temperatures (1.15 < T < 2.2 K) in order to study the effect of the normal fluid.

The chemical-potential difference is created by a displacement of a plunger moving at different constant velocities. We observe a sharp transition from subcritical to critical flow for all temperatures. Above the critical value we have two regimes: For high level differences (2 mm or more) the flow rate reaches a nearly constant value of about 40 cm/sec for a 20- μ hole; below this level difference one measures a smaller velocity, and the critical value obtained for a very small difference in levels is $v_c = 25 \pm 5$ cm/sec.

Finally we have studied the effect of a quartz transducer on the dc Josephson current; the critical current is strongly reduced for low voltages applied to the quartz; one can reach a cancellation of the flow for a critical voltage. For higher quartz excitation its own pumping action is predominant.

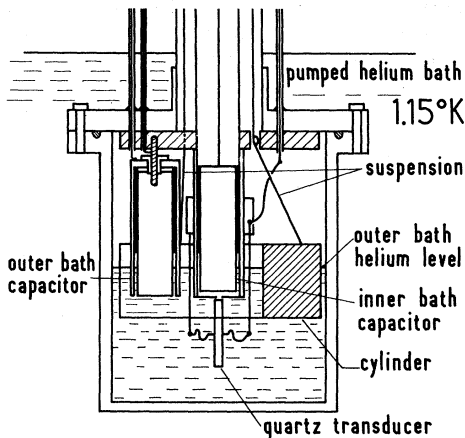


FIG. 1. Schematic diagram of the system used to measure the flow through the orifice placed at the bottom of the inner-bath capacitor.

This effect is similar to the influence of microwave power on superconducting junctions. The ac flow imposed by the quartz reduces the critical flow necessary to move vortices.

II. EXPERIMENTAL

A. General Description

A nickel foil ($15\ \mu$) with a coupling hole in its center ($15\text{--}20\ \mu$) is soldered at the bottom of the outer electrode of a cylindrical capacitor; the inside of this capacitor defines one helium bath whose level can be measured within $3\ \mu$. Another capacitor, open at the bottom, measures the level of the outer bath. These two capacitors are identical in the spacing between electrodes, equal within 1%. A metal plunger is partially immersed in the outer bath; its up-and-down motion provides a steady movement of the outer level. The setup is entirely contained in a sealed chamber filled at the beginning of the experiment (Fig. 1). This chamber is immersed in a pumped helium bath whose temperature is regulated. The Dewar is isolated from mechanical vibrations: The connections between the Dewar and the floor and walls of the room are made using low-pass mechanical filters consisting of lead weights and rubber plates and tubes; the pump is placed 10 m away with a large ballast volume to avoid pumping fluctuations.

B. Inner-Bath Capacitor

This is the most critical part of the experiment, and we will describe it thoroughly and critically. The main problem here is to keep the outside and inside bath temperatures as close as possible.

Our first design was a capacitor open at the very top, and similar to that of Richards or Khorana [Fig. 2(a)]. The outer brass electrode is soft sol-

dered to a thin-wall stainless-steel tube open at the top, but long enough to avoid a helium-film connection between the cylindrical electrodes. The inner electrode is soldered to the center conductor (0.05 mm diam) of a stainless-steel coaxial cable (0.5 mm diam) to avoid stray capacitance. Two rigid coaxial cables (1.2 mm diam) are used at the top as the measuring cables; they are grounded to the pot. The system's general shield thus includes the sealed pot and the outside electrodes of the two measuring cables.

As we said before, this type of condenser is not tight on top, the Teflon plug fits loosely to the stainless-steel tube, thus inside the tube the main part of the helium-film evaporation goes back down and recondenses; we thus avoid large helium leaks to the outside bath.

However, the condensation of the gas produces a heat flow which we estimate to be of about 2×10^{-4} W. The thermal contact between the two baths is not perfect and is, in our case, mainly limited by the Kapitza resistance. It results in a temperature difference of about 10^{-4} K. This ΔT creates at equilibrium a level difference of about 2 mm at 1.15°K , and 1 cm at 1.7°K ; this is a severe limitation. Furthermore, under this fountain pressure a normal fluid flow appears, compensated by a superfluid counterflow. These effects perturb our critical-flow study.

The interest of this design lies in the connection

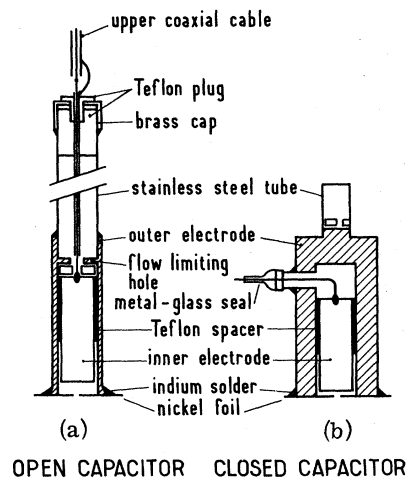


FIG. 2. Two types of capacitor used: (a) Open capacitor: the stainless-steel tube is 9.6 mm i.d., 10 mm o.d., and 370 mm long; the brass outer electrode is 9.6 mm i.d., 11 mm o.d., and 41 mm long; the flow-limiting hole is 3 mm i.d.; the inner electrode is 9 mm o.d. and 30 mm long. (b) Closed capacitor: the outer electrode, made out of electrolytic copper is 20 mm o.d., 9.6 mm i.d., and 38 mm long; the inner electrode is 9 mm o.d. and 20 mm long.

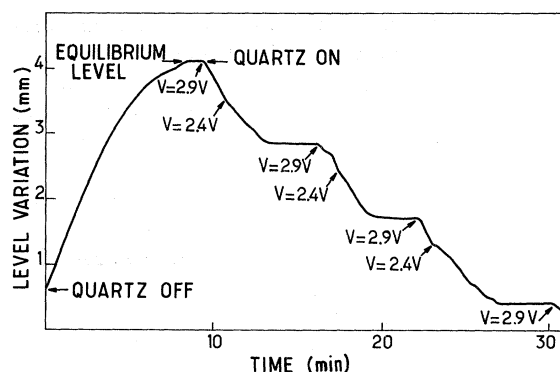


FIG. 3. Liquid-He head vs time due to the pumping action of transducer of frequency 127 kHz. Transducer voltage is momentarily increased to 2.9 V at points marked by arrows to kick the level out of the steps and then put back to 2.4 V.

between the gas of both baths at the top of the tube; it is then easy to define the chemical-potential difference as the energy lost by an atom going from one bath to the other through the gas. This will create a problem for our second system consisting of a completely closed capacitor [Fig. 2(b)].

The inner bath is connected to the outer one through the coupling hole only. A leak-proof metal glass seal is used for the electrical connection of the inner electrode. The capacitor is entirely at helium temperature, and the heat leaks of the film disappear completely. The outer electrode is made of thick electrolytic copper (5 mm) in order to get a uniform temperature. The capacitor is attached to the top of the sealed pot by a thin-walled tube. The top of the pot is slightly colder than the outer bath, and this could lead to temperature gradients. In our design, no sizable level difference appears between the two baths for any temperature between 1.15 and 2.26 °K.

However, this type of capacitor presents some limitations: When there is a helium flow inside the capacitor the rise of the helium level will cause some gas to condense in order to keep the vapor pressure constant; a temperature difference appears between the baths, due to the heat flow compensating the latent heat. This effect increases with temperature, and at the λ point the level difference is less than 5×10^{-2} mm and is easily taken into account as its variation is linear with the flow rate. Therefore, within our experimental limitation, the main drawback of our capacitor is that it is no longer possible to define the chemical-potential difference as the energy gained by an atom in its movement from one bath to the other through the gas. In order to test the identity between the chemical-potential and the level difference when the temperature is the

same on both sides, we reproduced the experiment of Richards and Khorana on the ac Josephson effect. The result is shown on Fig. 3. When the quartz transducer, placed in front of the coupling hole, is fed at its resonance frequency the inner helium level decreases and several stable steps appear; the distance between levels is, within 4%, equal to $h\nu/mg$.

C. Coupling Hole

We use 10- to 20- μ -thick nickel foils obtained by depositing electrochemical nickel on a metal plate with a 30- μ insulating mask in the middle.¹¹ Nearly round holes are obtained (Fig. 4), their diameter depending on the thickness of the deposit (10–20 μ). One side of the hole is conical and the other flat. The foil is very thin, and great care is taken to keep it flat. Let us note that it takes 2–3 min to evacuate the gas inside a closed capacitor through the hole. The pot must be pumped slowly to avoid the appearance of excessive pressure on the foil.

D. Plunger Mechanism

The metal cylinder is attached to three tergal strings; the strings are guided by pulleys placed at the top of the sealed pot, they prevent possible oscillations of the plunger placed at the end of long strings. The up-and-down movement is driven by an interchangeable synchronous motor.

E. Temperature Regulation

We pump helium down to 1.15 °K, the pumping circuit going through a large ballast volume to avoid pumping fluctuation. By controlling the pumping speed we get a rough temperature adjustment. The

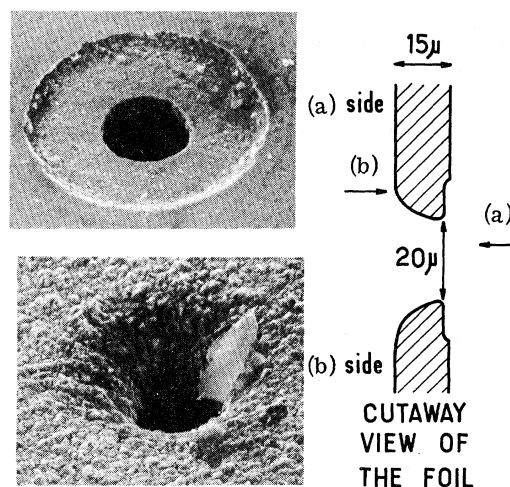


FIG. 4. Photographs of both sides of nickel foil obtained from an electron-scanning microscope, angle of view 45°.

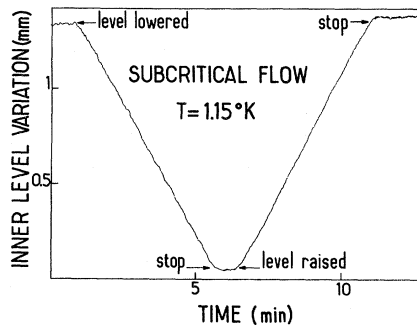


FIG. 5. Variation of inner-bath level due to up-and-down motion of the cylinder at low speed. Arrows indicate start and stop of the cylinder motion.

helium bath outside the experimental pot is then temperature regulated by the classical-pair heater Allen-Bradley measurement resistance.¹² We use a GR 1608 A bridge and JB 4 PAR lock-in detector whose output is fed to the heater through a dc amplifier. The temperature stability is about 10^{-5} °K below the λ point and 10^{-3} °K above.

F. Measurement

The flow is measured by a recording of the change in the capacitor when helium flows in and out; our electronic is similar to the one used by Richards.² One measures the off balance of a GR 1615 A bridge using a lock-in PAR HR 8 and a Moseley 7000 AM recorder. The precision, or the noise level, is about 3μ . The outer bath level is simultaneously measured, precision 20μ , by a Wayne-Kerr B 224 bridge.

At the beginning of the experiment, the sealed pot is thoroughly pumped out for a day. We then transfer liquid nitrogen and liquid helium into the main bath, while the pot is connected with a helium gas bottle through a charcoal filter cooled at nitrogen temperature. We then pump on the main bath and condense liquid helium in the pot; we pump slowly and seal the pot when the level measured by the capacitor reaches the desired value.

III. RESULTS

A. Low-Temperature Flow Study

Below 1.2 °K the normal-fluid component is small enough to be neglected in first approximation; we do the experiment by moving the plunger up and down at constant velocity, which thus acts as a variable current generator. We measure the helium levels of the two baths and study their variation with time when the plunger moves at different constant speeds between the two levels. The typical outside level variation lies between 1 and 0.1 mm/min. We can thus trace the flow-vs-gravitational potential. When

the cylinder motion is slow enough, the capacitance variation of both levels starts and ends simultaneously with the plunger movement. We thus observe a current at zero gravitational chemical-potential difference. We record the change with time of the capacitance. In Fig. 5 we show a typical recording for subcritical flow; let us note that the "level-raised" part of the flow curve is smoother than the "level-lowered" part: In the level-lowered part the plunger is lifted and is more sensitive to the irregularities of the driving motion.

If we increase the flow rate above a critical speed of the plunger, a level difference arises between the two baths; this critical velocity is $v_c = (25 \pm 5)$ cm/sec for a $20\text{-}\mu$ hole. Furthermore, when we stop the motor, the inner-bath level continues to move (Fig. 6). We can then trace the flow rate vs chemical-potential difference up to 3 mm.

The following are the main observations: (i) With a closed capacitor we get similar results for the two flow directions; when one uses the open capacitor, there is a marked dissymmetry between the two flow directions of about 20%, therefore we did not use it for this experiment. (ii) The helium flow stops rather abruptly when the equilibrium level is reached (Fig. 6); this is a characteristic of nonviscous flow. The limiting slope of the curve at zero level difference gives the critical velocity. (iii) When we are at supercritical velocity, the flow rate varies with level difference. We have about three regimes, shown on Fig. 7, for the low-temperature curves (1.13 and 1.57 °K): above 2.5 mm and up to 5 mm, which is the limit of our experimental head difference, the flow is almost constant with height difference; below 2.5 mm, it changes with head difference with a constant slope; very close to zero level difference one often ob-

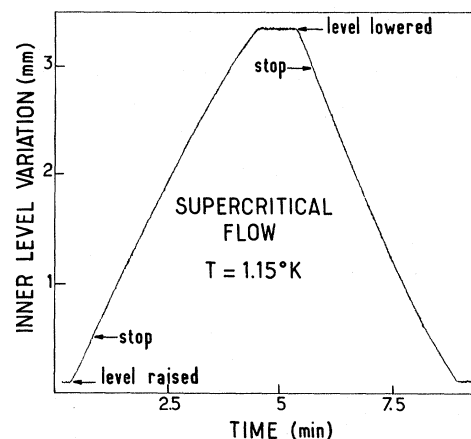


FIG. 6. Variation of inner-bath level due to down-and-up motion of the cylinder at high speed. Arrows indicate start and stop of the cylinder motion.

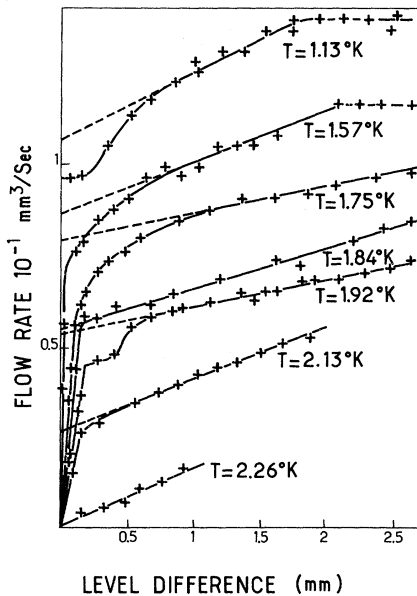


FIG. 7. Flow rate vs level difference obtained with a $20\text{-}\mu$ hole at various temperatures.

serves a very fast increase in the critical velocity of about 10%.

B. Variation of the Flow Rate With Temperature

We have repeated the experiment at different temperatures ranging from 1.15 to 2.26 °K, the results are presented on Fig. 7. Above the λ point, the flow rate is proportional to the level difference; This indicates a normal liquid flow; the flow impedance of the hole is then measured. A head difference of 1 mm produces a flow rate of 1.6×10^{-2} mm³/sec at 2.26 °K. Below the λ point, there is an abrupt change in the flow regime with a very strong increase of the flow for small level differences; this is a clear indication of the presence of a superfluid component, but it is only below 1.5 °K that one observes a flow with zero gravitational-potential difference within experimental limits.

These temperature experiments show that the subcritical flow exists under zero chemical potential, and that in the chemical potential the temperature term is important. When the proportion of normal fluid is large enough, any flow leads to a temperature difference between the two baths, and this is compensated by a level difference such as to maintain the total chemical-potential difference equal to zero.

We observe, for any temperature below the λ point, a critical flow; this flow varies linearly with the superfluid component density as expected (Fig. 8); the superfluid critical velocity is temperature independent.

IV. INTERPRETATION

A. Low-Temperature Case

In this temperature range the thermal effects are much reduced; the percentage of excitations is low (2–3%), and the normal flow can be neglected. A sharp transition is observed between nondissipative- and dissipative-flow regime (Fig. 7). The dissipation is due to the motion of vortices across the hole.

Let us recall the theory of a weak link in the ideal case.¹³ In a superfluid bath, the majority of atoms are in a single quantum state. They can be described by a type of macroscopic wave function¹⁴ or "order parameter" $\psi = \psi_0 e^{i\phi(r,t)}$. In a classical fluid the quantum phase varies randomly from one atom to another, here the variation of $\phi(r,t)$ is smooth on macroscopic distances. If the bath is set in motion with a local superfluid velocity \vec{v}_s , a phase gradient appears and

$$\vec{v}_s = (\hbar/m) \text{grad}\phi, \quad \text{rot } \vec{v}_s = 0. \quad (1)$$

Therefore, a superfluid motion is necessarily irrotational.

Let us take two baths (I and II), connected by a weak link like a small hole. If a current is induced between the baths, the superfluid velocity, and hence $\text{grad}\phi$, will be negligible outside the hole. The phases ϕ_I and ϕ_{II} of the two baths are well defined, and the difference $\phi_I - \phi_{II}$ is localized at the hole. If no current exists through the hole, $\phi_I = \phi_{II}$. For sufficiently low currents, $\phi_I - \phi_{II}$ remains constant with time: No pressure difference is necessary to drive the current as the superfluid is not viscous, and no dissipative mechanism occurs.

Above a critical current a pressure difference appears between the baths: The dissipative mechanism is not viscosity but the appearance of vortex motion through the hole. Vortices have a normal core of atomic size around which the superfluid is rotating; they can have the shape of lines stretched

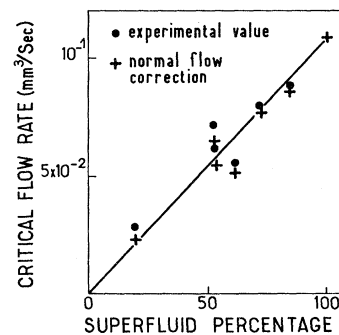


FIG. 8. Variation of critical-flow rate at various temperatures. The normal-flow correction is caused by the stray level difference appearing in the subcritical regime.

across the hole, or of rings (Fig. 9). $\text{rot } v_s$ is not zero on the core, and the velocity circulation around the vortex is quantized:

$$\int v_s dl = (\hbar/m) \int \text{grad} \phi dl = n h/m = n \kappa, \quad (2)$$

where κ is the circulation quantum, and m is the helium atom mass. Vortices carry kinetic energy: In an ideal weak link all the potential energy coming from the flow of helium under a nonzero pressure difference will be converted into vortex kinetic energy.

Let us give some crude arguments about the number of vortices created per unit time¹⁵: One assumes that vortices are in the shape of rings created near a wall [Fig. 9(b)], and grow as they gain energy from the pressure difference, so that they reach the radius b of the hole.

Using the impulse and energy conservation for a quantized vortex ring, Zimmermann¹⁵ finds the number of vortices created per unit time:

$$\nu = mg\Delta z/h. \quad (3)$$

He also calculates the superfluid critical velocity through the hole of radius b , assuming that singly quantized vortex rings¹⁶⁻¹⁹ of the same radius b are emitted. If a is the vortex core radius then we find

$$v_s = \frac{h}{mb} \left[\ln \frac{8b}{a} - \frac{7}{4} \right] \quad (4)$$

for $b = 10 \mu$, $v_s = 1.6 \text{ cm/sec}$.

Equations (2) and (3) have a deeper quantum-mechanical meaning if we use the phase of the order parameter. Let us consider two points A and B on each side of the foil, and a vortex ring outside the hole, as presented in Fig. 9(b). Circulation of $\nabla\phi$ along the sketched curve is equal to 2π for a singly quantized vortex. When the vortex is small, nearly all paths between A and B go around the vortex; when it has reached the radius b they all go inside it, and the circulation of $\nabla\phi$ is greater by 2π . The growing of a vortex corresponds to a jump of phase

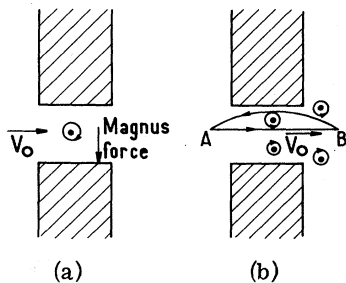


FIG. 9. Schematic of possible vortex motions through the hole: (a) corresponds to a pinned vortex line; (b) growth of a vortex ring under a flow velocity.

of 2π between the baths; the emission of ν vortices per unit time gives a phase variation rate of

$$\frac{d\Delta\phi}{dt} = -2\pi\nu = \frac{-mg\Delta z}{\hbar};$$

hence

$$\hbar \frac{d(\Delta\phi)}{dt} = -\Delta\mu = -\frac{\partial H}{\partial n}. \quad (5)$$

$\Delta\mu$ is the chemical-potential difference which is the energy variation when one atom is moved from one bath to another. H is the energy of the system.

The energy of a vortex is the energy change of the system when the phase variation is 2π ; it can be considered as $2\pi \partial H / \partial(\Delta\phi)$, hence

$$\hbar \frac{dn}{dt} = \frac{\partial H}{\partial(\Delta\phi)}. \quad (6)$$

Equations (5) and (6) were first introduced by Anderson.¹⁶ They imply that n and $\Delta\phi$ are conjugate quantum variables and are called Josephson-Anderson equations. The shape of the $I-V$ curve in the ideal case can be deduced from these equations.

In the subcritical regime with no vortex motion, the phase difference is constant with time for a constant current through the hole

$$\frac{d\Delta\phi}{dt} = 0 = \Delta\mu.$$

The phase difference between the baths increases as the current increases and if both baths are at the same temperature, no level difference appears.

In the supercritical regime, for a given level difference the rate of vortex emission is constant, and a linear increase of the phase difference appears with time.

It is clear from Eq. (5) that a difference in chemical potential is related to a change of the phase difference with time. This can be obtained by the notion of phase slippage introduced by Anderson, and related to the motion of vortices as we have just shown. Another possibility is simply a temporary acceleration of the superfluid without reaching the critical velocity. This is practically what happens when the level difference between the two baths comes back to equilibrium; oscillation of the levels must appear with an amplitude such that the velocity remains subcritical. The period can be derived from Eqs. (5) and (6).

The relation between the current and the velocity is

$$J = J_0 v_s / v_{0s};$$

v_s is the velocity in the smallest section of the coupling hole; J_0 and v_{0s} are the critical current and velocity. Assuming that in subcritical regime the phase difference $\Delta\phi$ remains proportional to v_s when J varies, let us define a thickness d of the hole

such that

$$\hbar \Delta\phi = mv_s d;$$

the relation between the current and the phase difference becomes

$$J = J_0 \Delta\phi / \Delta\phi_0,$$

where $\Delta\phi_0$ is the phase difference at which vortex motion appears. We have the two equations

$$\begin{aligned} \frac{\partial J}{\partial t} &= \frac{J_0}{\Delta\phi_0} \frac{\partial \Delta\phi}{\partial t}, \\ mg \Delta z &= \hbar \frac{\partial \Delta\phi}{\partial t}, \end{aligned} \quad (7)$$

then

$$\hbar \frac{\Delta\phi_0}{J_0} \frac{\partial J}{\partial t} = mg \Delta z$$

or

$$\hbar \frac{\Delta\phi_0}{J_0} \rho_s S \frac{\partial^2 z}{\partial t^2} = mg \Delta z,$$

where S is the area between the two circular sections of the capacitor.

The oscillation frequency of the levels is then

$$\omega^2 = mg J_0 / S \rho_s \Delta\phi_0 \hbar,$$

but

$$J_0 = \pi b^2 \rho_s v_{0s},$$

$$\hbar \Delta\phi_0 = m d v_{0s},$$

so

$$\omega = (\pi b^2 g / d S)^{1/2};$$

for $d \approx 30 \mu$, the corresponding period is $\nu \approx 2$ sec, and the maximum amplitude of level oscillations is $\Delta z \approx 10 \mu$.

In the experiment reported here, we have observed an abrupt stop of the level difference at equilibrium; this abrupt disappearance of the kinetic energy involves a dissipative process associated with the normal fluid, and will be analyzed in the next paragraph. We have recently observed these oscillations working at a temperature of 0.3 °K; they are analogous to the plasma oscillations introduced by Josephson for superconductors.

Let us now compare our experimental results with the simple Josephson theory. We demonstrate the existence of a finite critical velocity at low chemical-potential difference. Its value (25 cm/sec) is much higher than the calculated one obtained (1.6 cm/sec). It is also much higher than the value deduced by Richards.² However, his experiment was not aimed at the study of the critical velocity and, for low level difference, he does not observe any clear one, possibly because of temperature effects.

The typical calculations of a critical velocity are

valid for a long capillary where no end effects exist. In our case, because of the presence of image-force terms, the energy necessary to extract a vortex will be higher than the free energy. Besides the formation of the vortex itself is not clear; vortex rings may start as vortex lines trapped in the hole, and when the flow goes through, the line experiences a Magnus force perpendicular to it and to the velocity field [Fig. 9(a)] of value $\rho_s \vec{v} \times \kappa$ per unit length, which bends the line and, if the bending is sufficient, a vortex ring may appear.

This experimental value of 25 cm/sec is a lower limit of the supercritical flow rate. It rises quickly to values of about 35 cm/sec for about 1-mm level difference; we have noticed that this value is more reproducible from experiment to experiment than the first critical one. It seems that the first vortices originate from vortex lines trapped in the region of maximum flow velocity near the edge of the hole, or irregularities of the foil. For a 1-mm level difference, about 10^5 vortices/sec must be created. As the creation time is finite, vortices will appear everywhere in the hole, and not only in a few particular places. The mean energy per vortex will be higher and not so dependent on the initial state of the bath.

For high level difference, more than 2 mm, the flow rate critical velocity tends to saturate to a value of about 45 cm/sec. This is a regime of strong interaction energy between vortices. The velocity of a free vortex ring of 20 μ diam is about 1 cm/sec. As they are carried by the main flow their velocity relative to the foil will be of the order of 30 cm/sec. The distance between one vortex and the next, for a level difference of 3 mm, will be about 1 μ . The mean distance between vortices is smaller than their radius, and the velocity fields of nearby vortices strongly interfere; this leads to an increase of the energy per vortex.

B. High-Temperature Case

To analyze the high-temperature results we take the two-fluid model²⁰ in which separate equations are used for the normal flow of velocity v_n and the superfluid flow of velocity v_s :

$$\rho_s \frac{dv_s}{dt} = -\frac{\rho_s}{\rho} \nabla P + \rho_s S \nabla T - F_s - F_{sn}, \quad (8)$$

$$\rho_n \frac{dv_n}{dt} = -\frac{\rho_n}{\rho} \nabla P - \rho_s S \nabla T - \eta_n \nabla \times \nabla \times v_n + F_{sn},$$

$$\rho = \rho_s + \rho_n. \quad (9)$$

S is the mean entropy, ρ_s and ρ_n are the superfluid and normal densities, η_n is the viscosity of normal flow, and F_{sn} describes the friction between the superfluid and the normal fluid in the supercritical regime,²¹ caused by the diffusion of the normal excitations on the vortex core. F_s takes into account

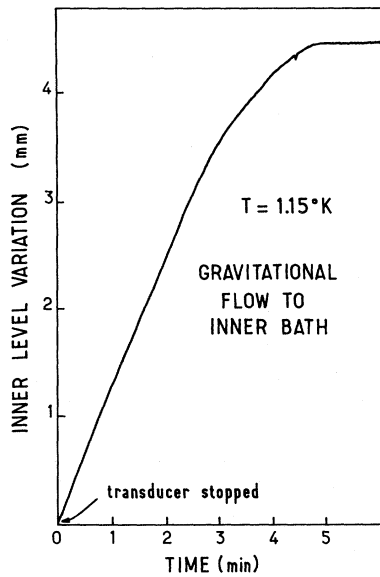


FIG. 10. Gravitational flow of liquid He II into the beaker ($T=1.15^{\circ}\text{K}$).

the energy given to the vortices during supercritical flow.

The volume integral of Eqs. (8) and (9) in a tube of current limited by the hole, linking the two baths, and long enough so that at its ends

$$\nabla P = \nabla T = v_s^2 = v_n^2 = 0,$$

gives, neglecting the acceleration,

$$-(\rho_s/\rho)\Delta P + \rho_s S\Delta T = (\langle F_s \rangle + \langle F_{sn} \rangle)d, \quad (10)$$

$$-(\rho_n/\rho)\Delta P - \rho_s S\Delta T = -Q_n/Z - \langle F_{sn} \rangle d. \quad (11)$$

Q_n is the volume flow rate of normal fluid, Z is the normal-flow impedance of the hole, $\langle F_{sn} \rangle$ and $\langle F_s \rangle$ are averaged values of F_{sn} and F_s taken on an average thickness d of the hole, where the velocity field remains significant.

Above the λ point, at 2.26°K , the measured flow rate of normal helium through the hole is $1.6 \times 10^{-2} \text{ mm}^3/\text{sec}$ for a 1-mm head difference. At lower temperatures, the normal flow varies with the viscosity η_n .

The curves presented in Fig. 7 show that above 1.5°K no flow under zero level difference is observed; the flow varies linearly with level difference up to a critical value. In order to give a physical explanation for this effect, let us consider a subcritical superfluid flow into the inner bath. The temperatures of both baths are then affected, for only the normal excitations carry entropy. In the stationary regime no chemical-potential difference will arise if a pressure difference is built up such that, from (10), $\Delta P = \rho S \Delta T$. The stationary regime

is reached when the heat leaks compensate the entropy flow towards the bath. They are related to the heat flow through the walls of the capacitors, limited by the Kapitza resistance, and a normal-fluid flow due to the level difference $Q_n = Z \Delta P$ from (11). One concludes that above 1.5°K the head difference no longer defines the chemical-potential difference; the normal-fluid contribution becomes important and leads to temperature differences, but one can still observe a subcritical flow under zero chemical-potential difference and a critical velocity. In Fig. 8, the critical-flow rates for different temperatures are plotted vs the corresponding superfluid densities. The ratio J_0/ρ_s is constant; we can thus conclude that the critical superfluid velocity is constant up to 2.13°K .

As one increases the level difference the flow-rate variation is rather similar to what is observed at low temperature. Above 2°K , the flow rate increases faster with head difference due to the contribution of the normal fluid. For example, at 2°K for about 2 mm of level difference, both flows are of the same order.

Thus at high temperatures the mixing of the superfluid flow and of the normal one, with similar orders of magnitude, does not allow one to consider the hole as a purely superfluid link. Good phase coherence experiments must be performed below 1.5°K .

V. EFFECT OF QUARTZ TRANSDUCER ON CRITICAL FLOW

In the Richards-Anderson² experiment a quartz transducer, placed close to the perforated nickel foil, is used to create an oscillating velocity field which synchronizes the vortex motion. In our experiment, a similar setup is used to study the variation of the critical flow, imposed by a moving plunger, as we vary the quartz voltage. We observe a very strong decrease and subsequent increase of the flow velocity with quartz potential.

We use a quartz frequency-control crystal type, driven at its longitudinal resonant frequency, 110–130 kHz. The rectangular end face, $1 \times 2 \text{ mm}$,

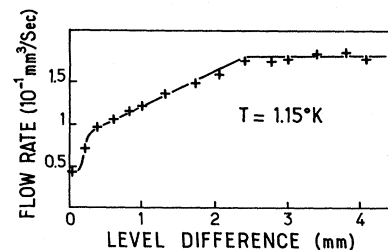


FIG. 11. Flow rate vs level difference obtained from gravitational flow.

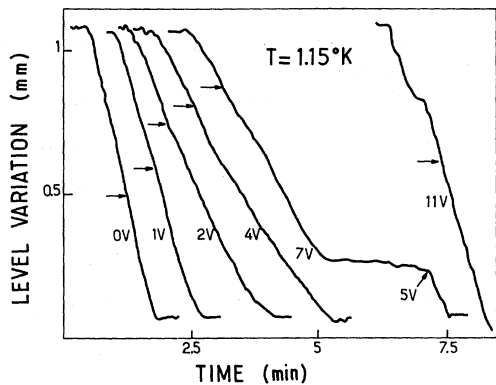


FIG. 12. Variation of inner-bath level due to up motion of the cylinder under various quartz voltages; arrows correspond to a stop of the cylinder motion.

is placed very close to the orifice (0.1–0.2 mm).

For a sufficiently large voltage applied to the quartz, about 5 V, a flow is induced from the inner bath to the outer one. Richards explains it by assuming that the transducer acts as a classical fluid pump. The fluid is driven along one side of the orifice; no Bernoulli pressure is obtained until vorticity is created between the quartz and the nickel foil.²²

After pumping, we study the decay of the head difference with time, the quartz turned off. A typical recording is shown on Fig. 10, and analyzed in Fig. 11. The initial critical velocity observed, 20 cm/sec, is lower than the one deduced from the preceding experiment; the maximum critical velocity 70 cm/sec is much larger. It thus seems that the presence of the quartz, very close to the hole, has a very important effect and drastically affects the critical velocity. The nickel foil and the quartz end face define a very small region with a very high density of vortices placed in front of the hole, and this changes markedly the flow dynamic.

Variation of Critical Velocity with Quartz Voltage

By analogy with the Shapiro²³ experiment on superconductors, we have studied how the flow under zero chemical-potential difference is affected by an oscillating current generated by the quartz. To create the dc flow we decrease the inner-bath level by an upward motion of the plunger placed in the outer bath, at a slightly supercritical velocity. The quartz is fed at different voltages during the plunger motion and afterwards. The results are

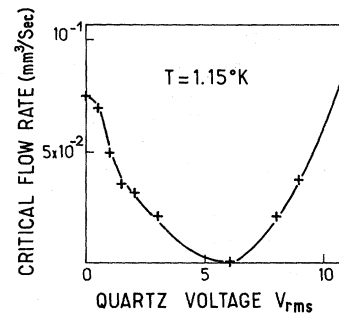


FIG. 13. Plot of flow rate extrapolated to zero level difference for various quartz voltages.

presented in Fig. 12. The critical velocity is first reduced and goes to zero for a quartz voltage of about 6 V, where the level cannot even reach equilibrium. For higher voltages, the pumping effect of the quartz becomes dominant, and the critical velocity increases again (Fig. 13).

Let us call $v_1 \cos \omega t$ the component of the induced velocity perpendicular to the foil, and v_0 the dc flow. If $v_0 + v_1$ is larger than v_{critical} during part of the ac period, vortices will be emitted and the critical velocity will be $v_c - v_1$ and not v_c . We will observe a decrease of the apparent critical velocity down to zero, and a subsequent increase as v_1 is increasing. If we assume that the velocity component perpendicular to the foil is of the same order of magnitude as the parallel one, it is reasonable to find that the critical velocity cancels out at about the voltage for which the quartz starts pumping.

VI. CONCLUSION

We have studied the dc Josephson effect in superfluid helium using for a weak link a small hole similar to the one used by Richards and Anderson in their classical experiment. By using a closed condenser and plunger, acting as a constant current source, we have been able to reduce temperature effects and avoid complex geometry imposed by a quartz. We have also shown how an ac flow can affect the dc critical current of the weak link. It appears also that the flow characteristics of the hole are affected by the presence of a quartz transducer placed in front of it. A detailed analysis of Richards and Khorana experiments should take into account the transducer-hole system as a whole. Experiments are now under way, with a similar system, at 0.3°K using a He₃ refrigerator.

¹B. D. Josephson, *Advan. Phys.* **14**, 419 (1965); P. L. Richards and P. W. Anderson, *Phys. Rev. Letters* **14**, 540 (1965); P. W. Anderson, in *Quantum Fluids*, edited by

D. F. Brewer (North-Holland, Amsterdam, 1966).

²P. L. Richards, *Phys. Rev. A* **2**, 1532 (1970).

³B. M. Khorana and B. S. Chandrasekhar, *Phys. Rev.*

- Letters 18, 230 (1967).
- ⁴B. M. Khorana, Phys. Rev. 185, 299 (1969).
- ⁵J. S. Langer and J. D. Reppy, in *Progress in Low Temperature Physics*, edited by C. J. Gorter (North-Holland, Amsterdam, 1970), Vol. VI.
- ⁶O. R. Williams and Marvin Chester (unpublished).
- ⁷H. A. Notarys, Phys. Rev. Letters 22, 1240 (1969).
- ⁸W. E. Keller and E. F. Hammel, Physics 2, 221 (1966); W. E. Keller, *Helium 3, Helium 4* (Plenum, New York, 1969), Chap. 8.
- ⁹W. J. Trela and W. M. Fairbank, Phys. Rev. Letters 19, 822 (1967).
- ¹⁰J. N. Kidder and W. M. Fairbank, Phys. Rev. 127, 987 (1962).
- ¹¹Obtained from Cacermet, Microformage, Raghénoplein 21, 2800 Mechelen, Belgium.
- ¹²C. Blake and C. E. Chase, Rev. Sci. Instr. 34, 948 (1963).
- ¹³R. J. Donnelly, Phys. Rev. Letters 14, 939 (1965).
- ¹⁴R. P. Feynmann in Ref. 5.
- ¹⁵W. Zimmerman, Jr., Phys. Rev. Letters 14, 976 (1965).
- ¹⁶P. W. Anderson, Rev. Mod. Phys. 38, 298 (1966).
- ¹⁷W. M. Hicks, Proc. Roy. Soc. (London) A102, 111 (1922).
- ¹⁸H. Lamb, *Hydrodynamics* (Dover, New York, 1945); G. W. Rayfield and F. Reif, Phys. Rev. 136, A1194 (1964).
- ¹⁹E. R. Huggins, Phys. Rev. A 1, 327 (1970); 1, 332 (1970).
- ²⁰L. D. Landau and E. M. Lifshitz, *Fluid Mechanics* (Pergamon, New York, 1959).
- ²¹W. F. Vinen, Proc. Roy. Soc. (London) A242, 493 (1957).
- ²²R. Meservey, Phys. Fluids 8, 1209 (1965).
- ²³S. Shapiro, Phys. Rev. Letters 11, 80 (1963).

PHYSICAL REVIEW A

VOLUME 5, NUMBER 4

APRIL 1972

Role of Electrostriction, Absorption, and the Electrocaloric Effect in the Stimulated Scattering of Light

P. Y. Key

Royal Holloway College, Englefield Green, Surrey, England

and

R. G. Harrison*

*United Kingdom Atomic Energy Authority, Research Group,
Culham Laboratory, Abingdon, Berkshire, England*

(Received 16 August 1971)

The modified hydrodynamic equations describing the behavior of a fluid under the influence of an optical electric field are solved. The contributions to stimulated scattering arising from electrostriction, absorptive heating, and the electrocaloric effect are exactly described. Previously unreported terms are given which significantly modify both the Rayleigh and Brillouin scattering. In particular, the experimentally observed stimulated Rayleigh scattering in non-absorbing media is shown to arise as much from electrostriction as from the electrocaloric effect, while anti-Stokes stimulated Brillouin scattering is predicted in a medium near its critical point. The possibility of observing additional scattering contributions proportional to $(\partial\epsilon/\partial T)_p$ is also discussed.

I. INTRODUCTION

Recent theoretical interest in stimulated Rayleigh scattering (SRS) and stimulated Brillouin scattering (SBS) has concentrated on establishing the profile of the nonlinear gain as a function of frequency shift.¹⁻⁹ The general theory describing the gain profile in an absorbing medium was originated by Herman and Gray¹ and developed by Starunov and Fabelinskii,^{3,4} who found that important modifications to that profile are indicated when the electrocaloric effect is taken into account.

In this paper we follow the above-mentioned authors in solving the hydrodynamic equations in the steady-state small-signal approximation,^{4,10}

i. e., assuming that the gain per wavelength of light is small and that the absorption coefficient for hypersonic is large compared with the gain. However, in solving these equations without further approximation, we have found new terms arising from electrostriction which contribute significantly to both SRS and SBS. The nature of the scattering contribution arising from the change in dielectric constant with temperature at constant density^{4,7} is also described and the possibility of observing such a contribution is discussed.

In order to clarify the role of the various physical effects involved in stimulated scattering, we present our results in a form in which the contributions arising from electrostriction, absorption, and the

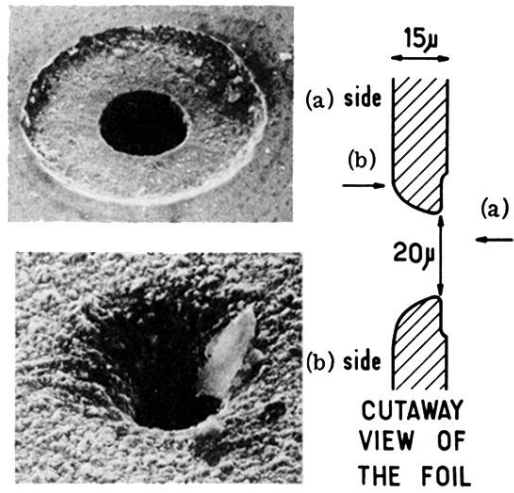


FIG. 4. Photographs of both sides of nickel foil obtained from an electron-scanning microscope, angle of view 45° .